Supporting Information

Electro-mechanical factor affecting the Li^+/Mg^{2+} selectivity performance of ion separation metal-organic frameworks

Yejin Lim[a,b,1], Youngoh Kim[a,b,1], Joonmyung Choi[a,b,]*

[a]*Department of Mechanical Design Engineering, Hanyang University, 222 Wangsimni-ro, Seongdong-gu, Seoul 04763, Korea*

[b]*Department of Mechanical Engineering, BK21 FOUR ERICA-ACE Center, Hanyang University, 55 Hanyangdaehak-ro, Sangnok-gu Ansan 15588, Korea*

[1] *These authors contributed equally to this work.*

Corresponding author

E-mail address: joonchoi@hanyang.ac.kr

Supporting Information

Table SI. Lennard-Jones potential parameters used.

Name	Description	σ (Å)	E (kcal/mol)	Ref.
Li	Lithium	2.13	0.0183	[1]
Mg	Magnesium	2.63	0.000956	[1]
Cl	Chlorine	4.42	0.118	[1]
Zr	Zirconium	2.78	0.069	[2]
O	Oxygen	3.12	0.06	[2]
C	Carbon	3.43	0.105	[2]
Hc	Hydrogen of UiO-66	2.57	0.044	[2]
N	Nitrogen	3.25	0.16979	[3]
Hn	Hydrogen of amine group	0	0	[3]
Hw	Hydrogen of water	0.4000	0.0460	[4]
Ow	Oxygen of water	3.1507	0.1521	[4]

Table SII. Composition of ionic solution and pure water.

Ionic Solution			**Puer Water**
Water	LiCl	$MgCl_2$	Water
5000	100	100	5000

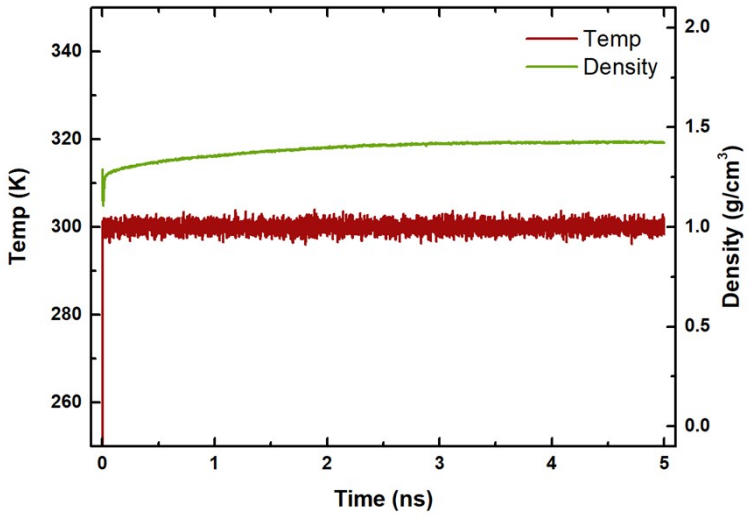

Figure S1. Convergence profiles of the temperature and density of the system over time under the NPT ensemble.

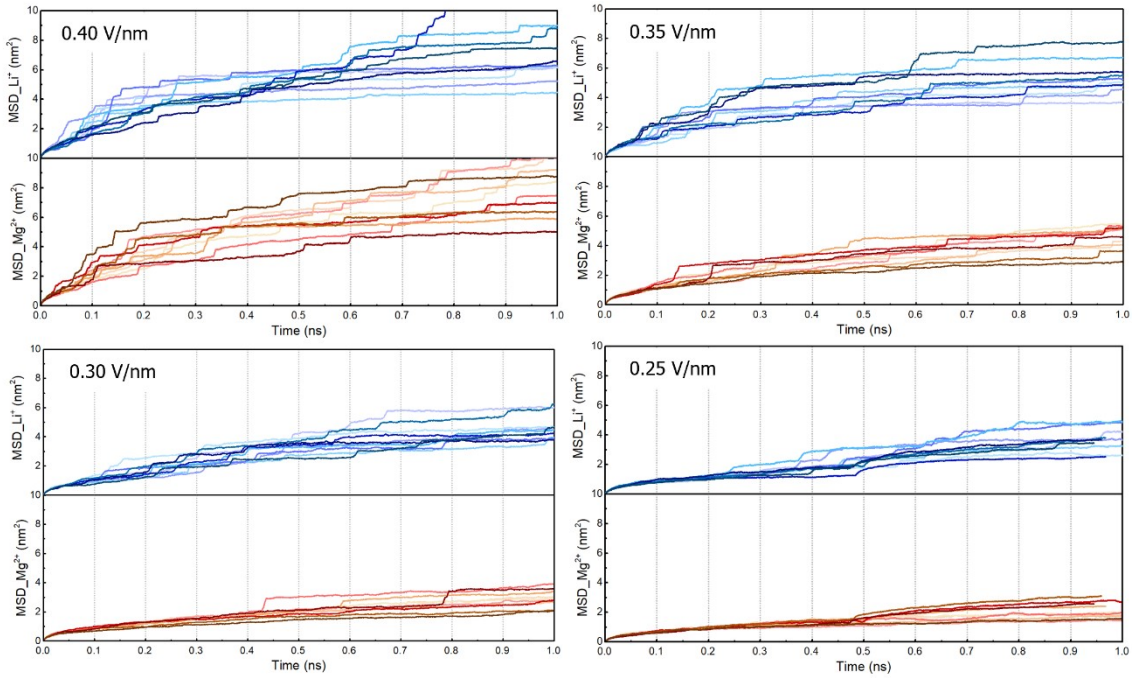

Figure S2 MSD curve of ions obtained by simulation repeated 10 times under electric field application conditions. The MSD curve of Li^+ shows a more frequent step-climbing behavior compared to that of Mg^{2+}, supporting the difference in the frequency of hydration shell collapse of the ions.

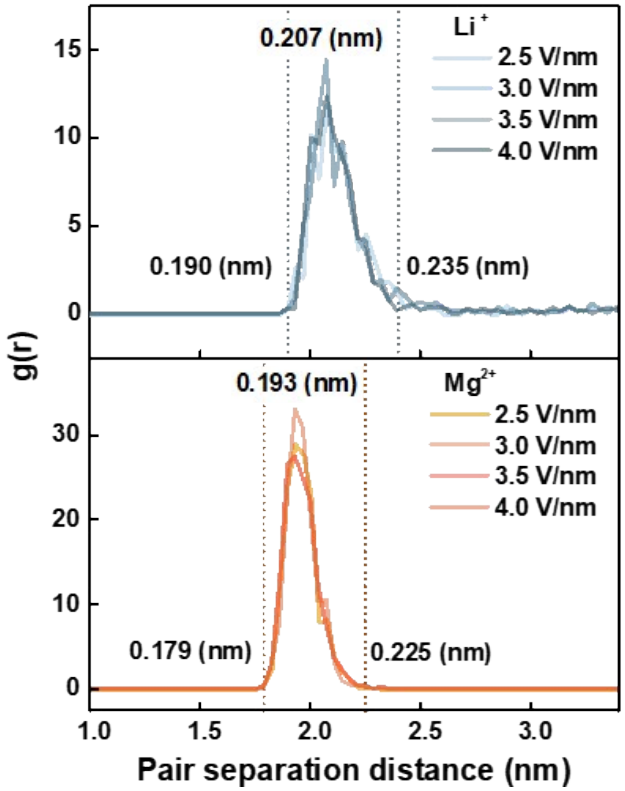

Figure S3. RDF curves of Li^+-O_{water} and Mg^{2+}-O_{water}. The area where the peak profile formed (indicated by the dotted lines) was set as the effective thickness of the first water shell.

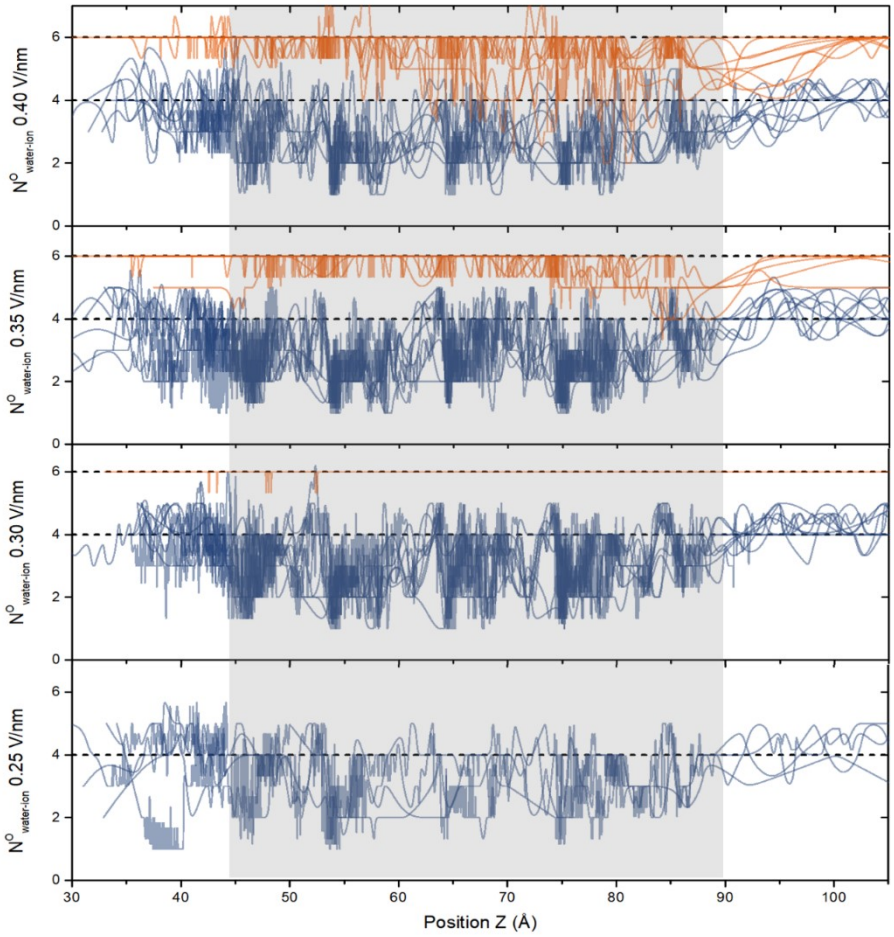

Figure S4. Ion-water ligand coordination number (N^O) changes according to the electric field strength. (Red: lithium, blue: magnesium, and gray box: UiO-66-$(NH_2)_2$ area)

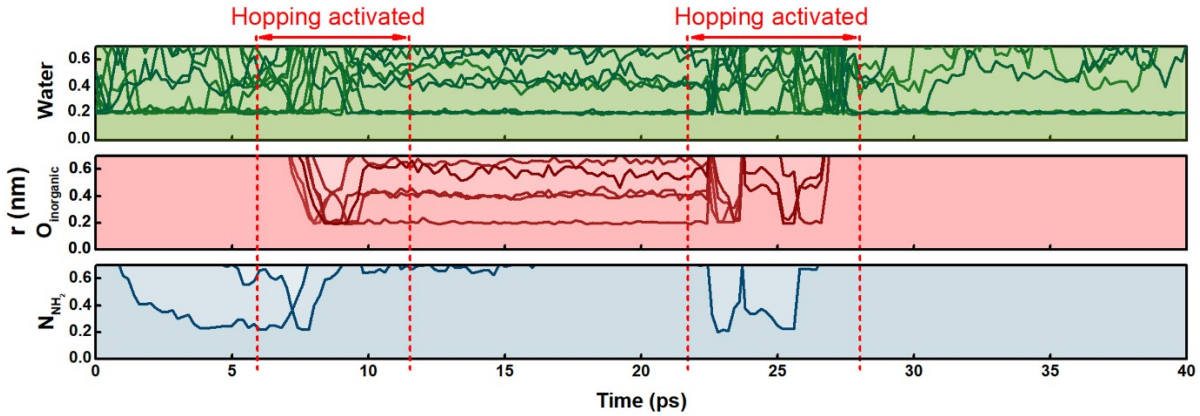

Figure S5. Results of classifying all hopping events of Li^+ ions according to the hopping type (green: water to water, red: water to inorganic brick, blue: water to amine hopping). At this moment, water-to-amine hopping was initiated, and immediately thereafter, the other two types of hopping were also significantly activated.

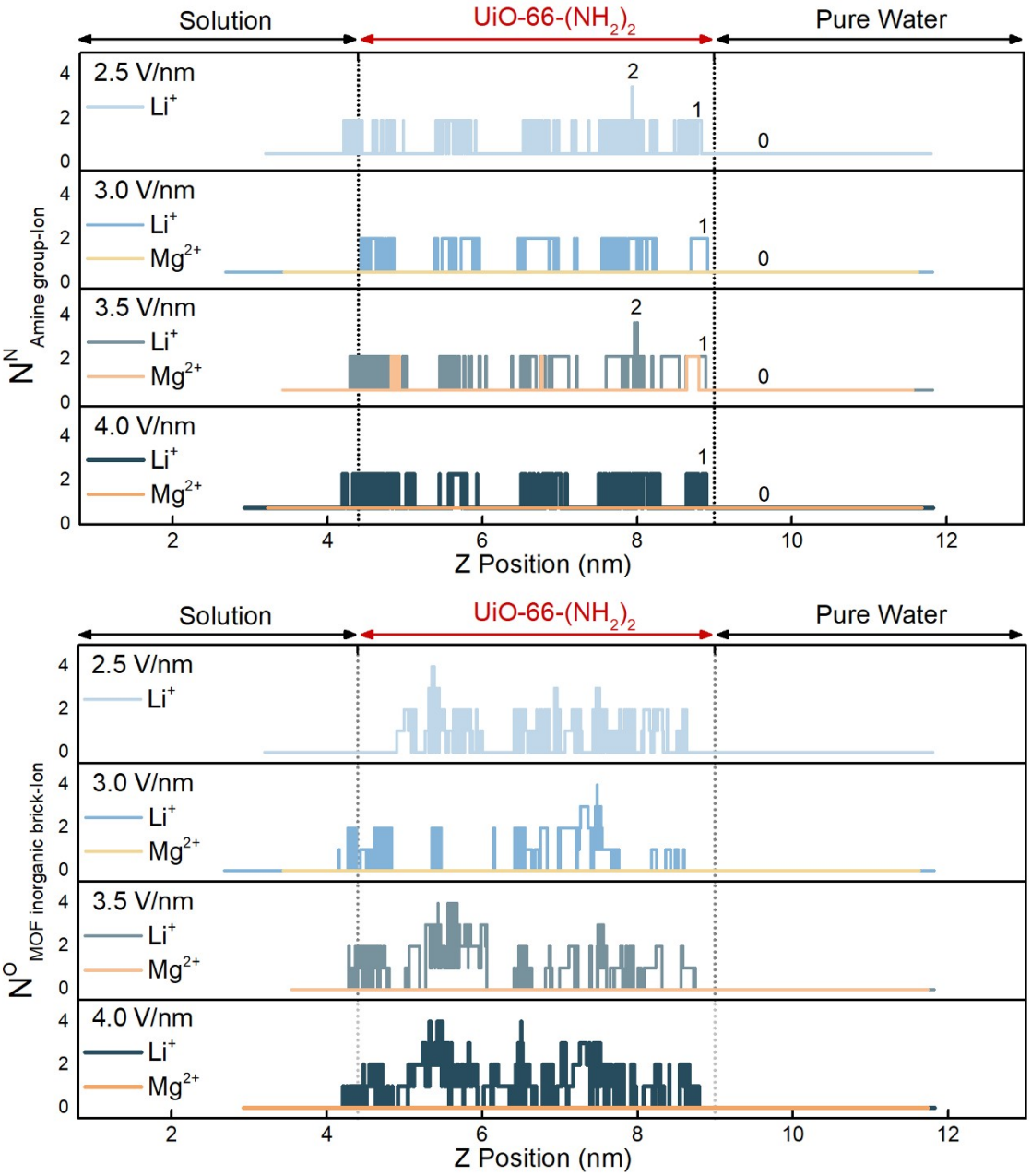

Figure S6 Contributions of **a.** amine group and **b.** inorganic brick on the ion hopping kinetics while passing through UiO-66-$(NH_2)_2$. The coordination number for nitrogen (N^N) of the amine group and oxygen anions (N^O) of the inorganic brick is considered for characterization of their involvement in the ion hopping kinetics.

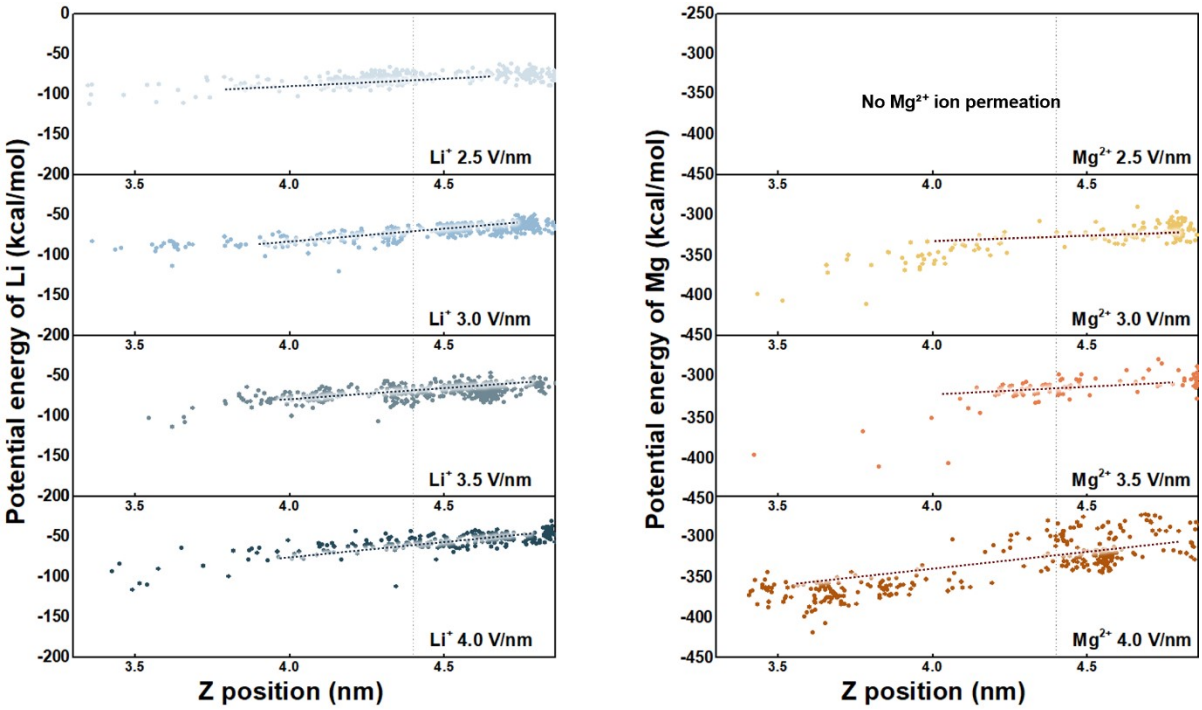

Figure S7. Potential energy distribution by the Z position of ions penetrating UiO-66-$(NH_2)_2$ during the simulation time.

References

1 X.-Y. Yue, Y.-Y. Li, Q.-W. Zhang, G. Liao and H.-B. Yi, *J. Mol. Liq.*, 2021, **327**, 114877.

2 S. K. Achar, J. J. Wardzala, L. Bernasconi, L. Zhang and J. K. Johnson, *J. Chem. Theor. Comput.*, 2022, **18**, 3593–3606.

3 A. Idrissi, M. Gerard, P. Damay, M. Kiselev, Y. Puhovsky, E. Cinar, P. Lagant and G. Vergoten, *J. Phys. Chem. B*, 2010, **114**, 4731–4738.

4 E. E. S. Ong and J.-L. Liow, *Fluid Phase Equilib.*, 2019, **481**, 55–65.